Some Aspects of Hurricane Inner-Core Dynamics and Energetics

KERRY A. EMANUEL

Center for Meteorology and Physical Oceanography, Massachusetts Institute of Technology, Cambridge, Massachusetts

(Manuscript received 26 December 1995, in final form 18 October 1996)

ABSTRACT

The energy cycle of the mature hurricane resides in the secondary circulation that passes through the storm's eyewall. By equating the generation of energy in this cycle to boundary layer dissipation, an upper bound on wind speed is derived. This bound depends on the degree of thermodynamic disequilibrium between the tropical ocean and atmosphere, on the difference between sea surface and outflow absolute temperatures, and also on the ratio between the enthalpy exchange and surface drag coefficients. Such a bound proves to be an excellent predictor of maximum wind speeds in two different axisymmetric numerical models and does not appear to depend on the existence of the hurricane eye. But further consideration of the detailed dynamics of the eye and eyewall show that the intensification of hurricanes is accelerated by feedbacks associated with a component of eye subsidence forced by radial turbulent diffusion of momentum. This radial momentum diffusion is an inevitable by-product of the strong frontogenesis that the author here shows to be a fundamental characteristic of flow in the eyewall. Thus, while the upper bound on hurricane wind speed is independent of the eye dynamics, the intensification of hurricanes is indirectly accelerated by turbulent stresses that occur in the eye and eyewall.

1. Introduction

Does the eye of a hurricane respond passively to processes operating in the eyewall or does it play an active role in the storm's evolution? This question was posed succinctly by Willoughby (1995) and lies at the heart of a general understanding of hurricane dynamics.

On the one hand, it is well known that the energy producing, thermally direct circulation resides in the in, up, and out secondary circulation that passes through the eyewall (Riehl 1950; Kleinschmidt 1951). The circulation in the eye is comparatively weak and, at least in the mature stage, thermally indirect, so it cannot play a *direct* role in the storm energy production. On the other hand, the temperature in the eyes of many hurricanes exceeds that which can be attained by any conceivable moist adiabatic ascent from the sea surface, even accounting for the additional entropy owing to the low surface pressure in the eye (Riehl 1954). Thus, the observed low central pressure of the storm is not consistent with that calculated hydrostatically from the temperature distribution created when a sample of air is lifted from a state of saturation at sea surface temperature and pressure.

Miller (1958) and, more recently, G. J. Holland (1997, manuscript submitted to *J. Atmos. Sci.*) explicitly consider subsidence warming as a contributor to low surface pressures in hurricanes. They estimate the amount of warming by calculating the temperature of a hypothetical air parcel descending through the eye and mixing with air from the eyewall. No attempt is made to ensure that the resulting temperature distribution is consistent with the thermal wind relation applied to a reasonable distribution of azimuthal velocity in the eye.

Smith (1980) pointed out that thermal wind balance restricts the amount of warming that can take place. In essence, the rotation of the eye at each level is imparted by the eyewall, and the pressure drop from the outer to the inner edge of the eye is simply that required by gradient balance. Because the eyewall azimuthal velocity decreases with height, the radial pressure drop decreases with altitude, requiring, through the hydrostatic equation, a temperature maximum at the storm center. Smith's model explicitly recognizes that the eye circulation of a mature storm is mechanically driven by the eyewall, as it must be if it is thermally indirect. The warmth of the eye relative to the eyewall, and the pressure drop to the center of the eye, are determined by the rotation of the eyewall, and to calculate this, no account of the details of the eye stratification or mixing with the eyewall is necessary.

Smith's account of the dynamics of the eye is supported by numerical integrations using the model of Emanuel (1995a). In that model, it is possible to arbitrarily specify the stratification experienced by dry descending air. Figure 1 shows that the maximum wind speed and minimum surface pressure achieved by model

Corresponding author address: Dr. Kerry A. Emanuel, Center for Meteorology and Physical Oceanography, Massachusetts Institute of Technology, Room 54-1620, Cambridge, MA 02139.
E-mail: emanuel@texmex.mit.edu

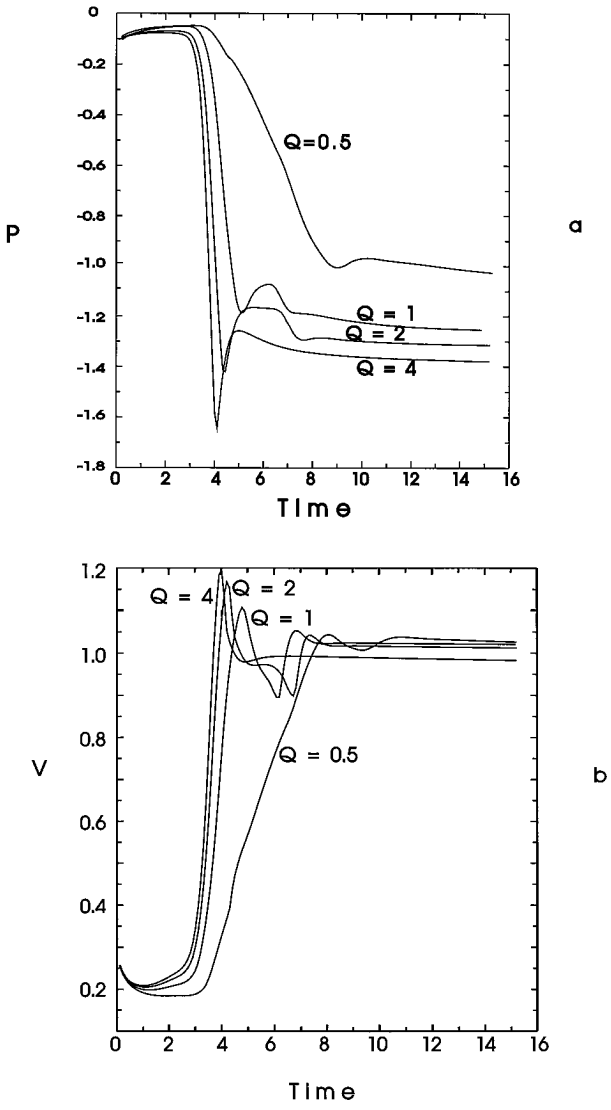

FIG. 1. (a) Central surface pressure and (b) maximum swirling velocity as functions of time for four values of the imposed dry stratification Q using the model of Emanuel (1995a). All quantities are dimensionless.

storms are largely independent of the value of the stratification (as long as it is not too small, i.e., $Q \lesssim 0.5$), confirming the predictions of Smith's theory.

Thus, given the swirling velocity of the eyewall, the steady-state eye structure is largely determined. But does the adjustment of the eye to the eyewall have any important effect on the spinup of the latter? This is essentially Willoughby's (1995) question.

An approach to estimating the maximum intensity of hurricanes was developed by the author (Emanuel 1995b). Detailed consideration of the subcloud-layer entropy budget of the eyewall region, together with an assumption about the subcloud-layer relative humidity just outside the eyewall and an assumption of slantwise convective neutrality, leads to a prediction of maximum wind speed that depends on the degree of ambient air–sea thermodynamic disequilibrium, the difference between the sea surface and outflow temperatures, and the ratio of the exchange coefficients of enthalpy and momentum. This estimate is independent of any consideration whatsoever of the eye. But the central pressure, which is estimated by integrating the gradient balance equation inward from the radius of maximum winds, does depend on the assumed radial profile of azimuthal wind in the eye. By assuming solid body rotation, both the maximum wind speed and central pressure are in excellent agreement with the results of numerical integrations using two quite different models.

All this would seem to imply that the eye is a purely passive response to the dynamics of the eyewall and outer region. The aforementioned work establishes that the energetic bound on maximum wind speed is indeed independent of the eye dynamics, but whether hurricanes are dynamically capable of achieving this bound has not been established. This spinup problem is largely the subject of the present work. After rederiving the upper bound on wind speed using an energy argument, simple nonlinear models of the eyewall evolution are used to demonstrate that the eyewall is an atmospheric front. These models imply that while the wind field can amplify purely from wind-induced surface heat exchange (WISHE), amplification of the entropy field depends on the interaction of hurricanes with external dynamical systems and/or on diffusive processes associated with frontal collapse of the eyewall. It is further demonstrated that these diffusive processes lead to more rapid intensification of the wind field than otherwise would occur. The results are summarized in section 4.

2. The energy cycle

In earlier work, the author (Emanuel 1986, 1988) considered the total amount of mechanical energy produced when a sample of air traverses the circuit indicated in Fig. 2. This amount of energy can be expressed as

$$\mathcal{E} = \epsilon T_s(s_c - s_a), \tag{1}$$

where s is the total specific entropy, given by

$$s = [c_{pd}(1 - q) + c_l q]\ln T + \frac{L_v q}{T} - [R_d(1 - q) + R_v q]\ln p, \tag{2}$$

and ϵ is the thermodynamic efficiency, where

$$\epsilon \equiv \frac{T_s - T_o}{T_s}. \tag{3}$$

In (2), c_{pd} is the heat capacity at constant pressure of dry air, c_l is the heat capacity of liquid water, q is the specific humidity, T is absolute temperature, L_v the latent heat of vaporization, R_d the gas constant of dry air, R_v the gas constant of water vapor, and p the pressure. The subscripts c and a refer to storm center and ambient

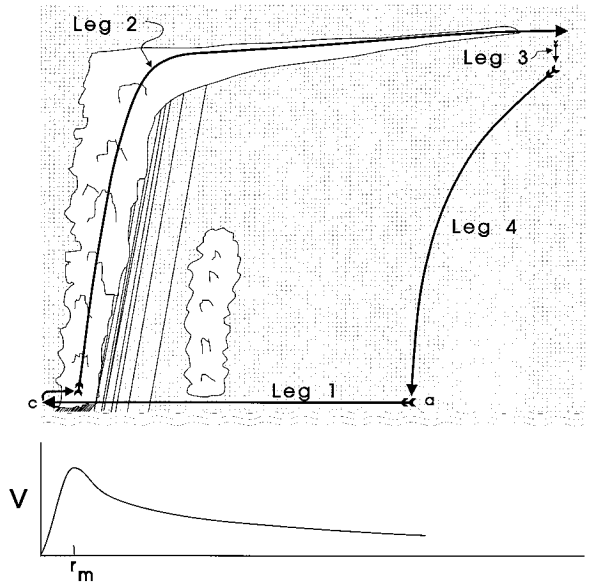

FIG. 2. Hypothetical air trajectory in the original Carnot cycle model (Emanuel 1986). Air flows all the way into the center, turns, and flows up through the eyewall. The swirling velocity profile is shown at bottom.

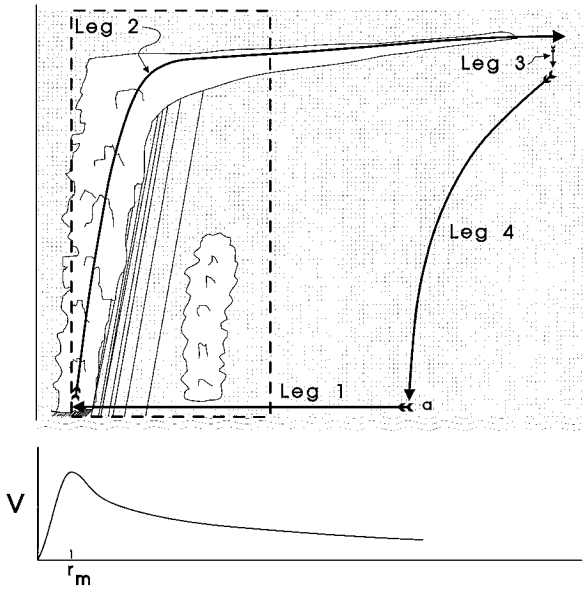

FIG. 3. Hypothetical air trajectory in a modified Carnot cycle. Air does not flow into the center but instead turns and flows up through the eyewall. The budget calculations discussed in text are performed inside the dashed box.

environment, respectively. In (3), T_s is the sea surface temperature and T_o the entropy-weighted mean temperature of the storm's outflow.

In order to find the minimum central pressure sustainable in a steady hurricane, the available energy given by (1) was equated with the frictional dissipation along the surface leg of the trajectory (Fig. 2) and the work dissipated in the outflow. The resulting estimates of minimum central pressure are in good agreement with the central pressures of the most intense storms observed (Emanuel 1988).

The trajectory considered in this analysis is problematic in that the inward spiraling air is carried all the way into the center of the storm. This is equivalent to assuming that the thermodynamic profile in the eye is moist adiabatic (Emanuel 1986; G. J. Holland 1997, manuscript submitted to *J. Atmos. Sci.*). Observations, on the other hand, often show a strong temperature inversion at low levels (e.g., Malkus 1958), with most (but not all) of the inflow turning upward at the eyewall. This was one of the bases of a recent critique of this theory by G. J. Holland (1997, manuscript submitted to *J. Atmos. Sci.*). Indeed, one of the predictions of the theory, that the minimum central surface pressure is independent of the value of the surface heat, moisture, and momentum exchange coefficients, is in poor agreement with numerical experiments (Ooyama 1969; Rosenthal 1971; Emanuel 1995b), which show a strong dependence of central pressure on the ratio of the surface enthalpy exchange coefficient to the surface drag coefficient. The fact that the prediction of central pressure is in good agreement with observations implies that the magnitude of the exchange coefficient ratio in nature is near or slightly larger than unity (Emanuel 1995b).

The problem of artificially including the eye in the energy cycle of the mature hurricane can be avoided by considering instead the *rates* of energy and entropy production and dissipation. Figure 3 shows the domain over which the budgets are calculated. Air is assumed to enter the domain in the frictional boundary layer and exit near the top of the outer boundary of the domain. No assumptions are made about the structure of the eye.

Once again, the mechanical energy available from the Carnot cycle is given by

$$E = \epsilon T_s \Delta s, \tag{4}$$

but here Δs represents the entropy increase from the outer boundary to the eyewall rather than to the center. The *rate* of mechanical energy production is

$$ME = M\epsilon T_s \Delta s, \tag{5}$$

where M is the mass flux of the secondary circulation. In equilibrium, this energy production must equal the dissipation in the system. For simplicity, we shall assume that *all* of the dissipation occurs in the frictional boundary layer. [Emanuel (1986) showed that in general, one must also account for dissipation in the outflow, but this is usually small unless the storm's radial dimension is quite large.] Thus,

$$M\epsilon T_s \Delta s \simeq \mathcal{D}, \tag{6}$$

where $\mathcal{D}$ is the rate of dissipation in the boundary layer. Considering that entropy is added to the atmosphere by the sea and momentum is lost to the sea, (6) may be expressed as

$$\int_{r_m}^{r_0} \rho\epsilon T_s C_k |\mathbf{V}|(s_0^* - s_b) r \, dr = \int_{r_m}^{r_0} \rho C_D |\mathbf{V}|^3 r \, dr, \quad (7)$$

where r_m is the radius of the eyewall (approximately the radius of maximum winds), r_0 is an outer radius, $|\mathbf{V}|$ is the surface wind speed, s_0^* is the saturation entropy of the ocean surface, s_b is the actual entropy of subcloud-layer air, ρ is the density, C_k is the coefficient controlling enthalpy fluxes from the ocean, and C_D is the drag coefficient.

We shall now assume that the largest contributions to both integrals in (7) come from the flow near the radius of maximum winds. In the first place, most of the actual entropy increase in the boundary layer occurs near the radius of maximum winds (Hawkins and Imbembo 1976). Also, as the dissipation varies as the cube of the wind speed, its dominant contribution will come from the high wind speed regions. Thus (7) may be written approximately as

$$|\mathbf{V}_m|^2 \simeq \frac{C_k}{C_D} \epsilon T_s (s_0^* - s_b)|_m, \quad (8)$$

where $|\mathbf{V}_m|$ is the maximum wind speed and the right-hand side is evaluated near the radius of maximum winds. [Note that (8) is not yet a *closed* expression for $|\mathbf{V}_m|$ as specification of $s_b|_m$ is required.[1]]

Although (8) is expressed as an approximation, its exact form was derived by the author (Emanuel 1986, 1995b) by considering the entropy balance of the subcloud layer in the eyewall under the assumption that entropy is constant along angular momentum surfaces there. That derivation [Eq. (13) of Emanuel 1995b] gives (8), but with the approximate equality replaced by an actual equality. The problem of determining the maximum wind speed is closed by specifying a value of the relative humidity of the subcloud layer just outside of r_m. This allows one to calculate both $s_b|_m$ and the pressure at r_m needed to calculate s_0^*. The maximum wind speed so estimated is compared to the results of simulations using two very different numerical models in Fig. 4. [The theoretical curve has been calculated assuming that the subcloud layer relative humidity just outside the eyewall is 80%. See Emanuel (1995b) for details.] Clearly, (8) gives an excellent estimate of the maximum wind speed and its correct dependence on C_k/C_D.

The derivations leading to (8) either from the present consideration of storm energetics or from the entropy balance of the subcloud layer (Emanuel 1995b) do not account in any way for the dynamics of the hurricane eye, suggesting that the dynamics has no important influence on the maximum wind speeds. On the other hand, one does need to know something about the eye to estimate the central pressure. The author showed that merely assuming that the eye is in solid body rotation and calculating the eyewall-to-center pressure drop from cyclostrophic balance gives an estimate of central pressure in excellent agreement with numerical simulations (Fig. 3 of Emanuel 1995b). This suggests that the eye can be regarded as a passive response to the eyewall, in which the eye rotation is imparted by turbulent flux of momentum from the eyewall, until the eye has attained approximately solid body rotation. This basic view of eye dynamics has been advanced by Smith (1980) and is supported by the angular momentum budget analysis of a numerical simulation by Kurihara and Bender (1982). In the next section, we examine whether the eye also acts as a passive partner during the intensification of the storm.

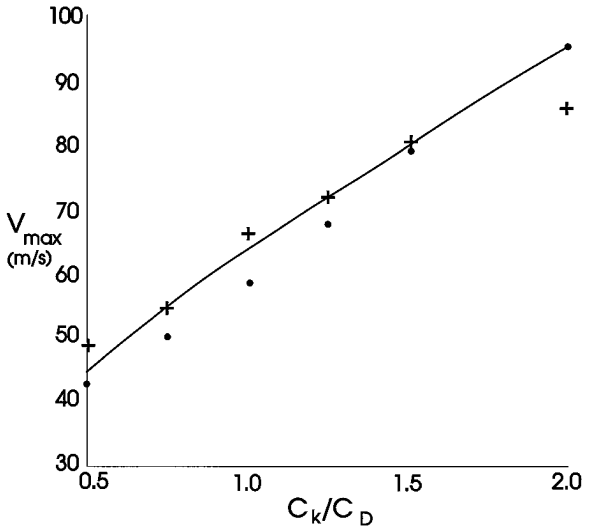

FIG. 4. Theoretical value of the maximum wind speed in fully developed tropical cyclones as a function of the ratio of the heat and momentum surface exchange coefficients. The dimensional values have been obtained using the scaling factors in Table 1 of Emanuel (1995a). The results of running the numerical model of Emanuel (1995b) are shown by dots, and those of running the model of Rotunno and Emanuel (1987) are shown by crosses. From Emanuel (1995b).

3. The eyewall as an atmospheric front

The hurricane eyewall is a region of rapid variation of thermodynamic variables. The transition from the eyewall cloud to the nearly cloud-free eye is often so abrupt that it has been described as a form of atmospheric front (e.g., Palmén and Newton 1969, 486). Eliassen (1959) was perhaps the first to recognize that the flow under the eyewall cloud is inherently frontogenetic. Here we show that a simplified form of the balance model presented by the author (Emanuel 1995a) indeed entails strong frontogenesis at the inner edge of the eyewall. Details of the derivations of the model

[1] The expressions in (7) and (8) do not account for dissipative heating in the boundary layer. This changes the denominator of (3) to T_0 and will be described in a forthcoming work by Bister and Emanuel.

equations presented here may be found in Emanuel (1995a).

The eyewall is a region of rapid ascent that, together with slantwise convection, leads to the congruence of angular momentum and moist entropy (θ_e) surfaces (Rotunno and Emanuel 1987). This directly implies that three-dimensional vorticity vectors lie on θ_e surfaces, so that the moist potential vorticity vanishes. As the air is saturated, this in turn implies, through the invertibility principle applied to flow in gradient and hydrostatic balance, that the entire rotational flow may be deduced from the radial distribution of θ_e in the boundary layer and the distribution of vorticity at the tropopause. The invertibility relation, equivalent in this case to a thermal wind relation, was derived by Emanuel [1986, Eq. (11)] and may be expressed in nondimensional form as

$$\frac{1}{r_b^2} = \frac{1}{r_t^2} - \frac{2}{R^3}\frac{\partial \chi}{\partial R}, \tag{9}$$

where r_b is the (nondimensional) physical radius of an angular momentum surface where it intersects the surface, r_t is the radius of the same surface at the tropopause, χ is the nondimensional entropy variable, and R is the nondimensional potential radius, which is proportional to the angular momentum per unit mass and is given by

$$R^2 = 2rV + r^2, \tag{10}$$

where V is the dimensionless azimuthal velocity. (See Emanuel 1995a for the scaling factors.) Equation (9) states that when there is a negative radial gradient of entropy in the boundary layer under the eyewall (equivalent to a negative radial gradient of temperature aloft), the radius of angular momentum surfaces at the surface must be smaller than it is at the tropopause, implying a negative gradient of azimuthal wind with altitude. Thus, (9) is a thermal wind equation.

The angular momentum surfaces in the eyewall of a mature storm typically flare out to large radius, except perhaps those that originate near the inner edge of the eyewall. If $r_t^2 \gg r_b^2$, then (9) may be approximated by

$$\frac{1}{r_b^2} \simeq -\frac{2}{R^3}\frac{\partial \chi}{\partial R}. \tag{11}$$

Furthermore, in the region of large winds, the contribution of the swirling velocity to the angular momentum is vastly larger than the contribution of the earth's rotation, and so the second term on the right of (10) (which is multiplied by f, the Coriolis parameter, in its dimensional form) can be neglected, giving

$$R^2 \simeq 2rV. \tag{12}$$

Combining (11) and (12) gives

$$V^2 \simeq -\frac{R}{2}\frac{\partial \chi}{\partial R}. \tag{13}$$

Thus, the square of the swirling velocity varies as the gradient of entropy with respect to potential radius in the eyewall region. Now it is important to be aware that the *only* radial flow in R coordinates is that owing to friction, since dR/dt (the radial flow in R space) is proportional to the rate of change of angular momentum. The dimensionless equation for angular momentum conservation is

$$\gamma\frac{dR}{dt} = -rV^2/R,$$

where γ is the nondimensional boundary layer depth (see Emanuel 1995a) and we have neglected the wind dependence of the surface drag coefficient. Using (10) in the cyclostrophic limit ($r \ll 2V$), this becomes

$$\gamma\frac{dR}{dt} \simeq -\frac{1}{2}RV. \tag{14}$$

These relations can be used to help understand the dynamics of the eyewall region, as illustrated in Fig. 5. Consider the eyewall to be a region of large negative gradient of χ, corresponding through (13) to large V^2. Regions of large V give rise to relatively large cross-R surface flow, which advects entropy (χ) across R surfaces. But since V [and thus, through (13), $\partial\chi/\partial R$] must vanish at $R = 0$, this implies that $-\partial^2\chi/\partial R^2$ will increase with time and thus, again using (13), $\partial V/\partial R$ must also

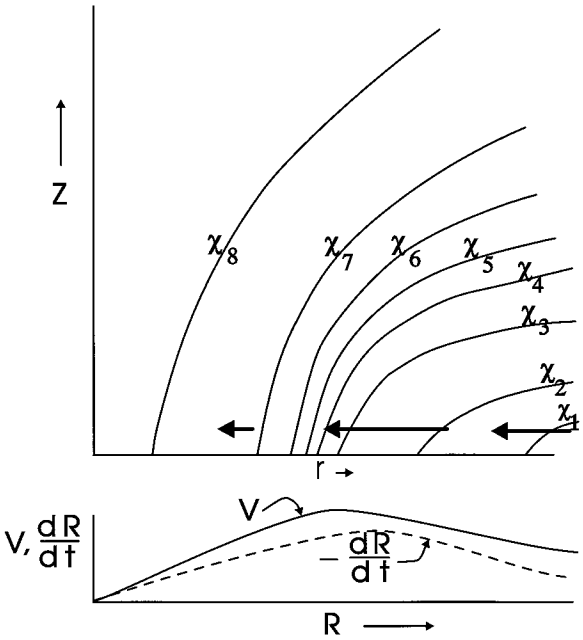

FIG. 5. Schematic distribution of entropy (χ) as a function of height and radius (r) in a developing tropical cyclone. Note that R is assumed to be constant along surfaces of constant χ. It is assumed that the storm is well enough developed that these surfaces flare out to large radius near the tropopause, corresponding to an anticyclone there. At the bottom is shown the distribution of swirling velocity, V, which is proportional to $\sqrt{-R(d\chi/dR)}$, and the time rate of change of potential radius, which is proportional to RV. This shows how surface friction leads to eyewall frontogenesis.

increase. The relative vorticity itself can be related to $\partial V/\partial R$ by using the definition of relative vorticity in cylindrical coordinates

$$\zeta = \frac{V}{r} + \frac{\partial V}{\partial r},$$

together with the coordinate transformation

$$\frac{\partial}{\partial r} = \frac{\partial R}{\partial r}\frac{\partial}{\partial R} = \frac{r}{R}\left(1 + \frac{V}{r} + \frac{\partial V}{\partial r}\right)\frac{\partial}{\partial R} = \frac{r}{R}(1 + \zeta)\frac{\partial}{\partial R},$$

where we have used (10). The result of combining these two expressions is

$$\zeta = \frac{\dfrac{V}{r} + \dfrac{r}{R}\dfrac{\partial V}{\partial R}}{1 - \dfrac{r}{R}\dfrac{\partial V}{\partial R}}, \tag{15}$$

so that a discontinuity forms when $\partial V/\partial R = R/r$. As in semigeostrophic theory, the actual secondary circulation leading to frontal collapse is implicit. In the classic semigeostrophic theory of deformation-induced frontogenesis (Hoskins and Bretherton 1972), the background geostrophic deformation flow provides the advection of temperature across surfaces of absolute momentum (the linear analog of angular momentum) that drives the frontogenesis, whereas in the hurricane eyewall, surface friction provides the cross-angular momentum surface advection of entropy. Also note that the hurricane eyewall is not necessarily a front in surface temperature, but instead involves the θ_e distribution, which is directly related to density in saturated air.

The above heuristic description can be approximately quantified by developing an equation for the entropy content, χ. In the eyewall region, χ does not vary appreciably along angular momentum surfaces, and the conservation equation for χ can be integrated upward along such surfaces to yield [Emanuel 1995a, Eq. (A6)]

$$\gamma\frac{\partial \chi}{\partial \tau} = \beta\left[\frac{1}{2}RV\frac{\partial \chi}{\partial R} + \frac{C_k}{C_D}V(\chi_0^* - \chi)\right], \tag{16}$$

where γ is the nondimensional depth of the boundary layer, C_k/C_D is the ratio of the surface enthalpy exchange to surface drag coefficients, and χ_0^* is the saturation entropy of the sea surface. The wind dependence of the surface exchange coefficients has been neglected in (16). The parameter β is included in (16) as a crude way of accounting for processes affecting the χ distribution outside the eyewall. These processes include convective and large-scale downdrafts, which import low θ_e air into the subcloud layer. The first term on the right-hand side of (16) is the advection of χ across R surfaces by the frictionally induced part of the radial flow, while the second term is the surface flux of entropy.

It is useful to pause at this point and review the assumption behind this simplified model of hurricane dynamics. First, we have assumed that the fields are axisymmetric, that the eyewall is saturated, and that entropy and angular momentum surfaces are congruent in the eyewall. We have assumed gradient and hydrostatic wind balance everywhere above the boundary layer and further assumed cyclostrophic balance near and within the radius of maximum winds. At the top of the storm, we have assumed that the circulation has been in existence long enough that an anticyclone has formed with approximately zero absolute vorticity. We have *not* assumed anything further about the thermodynamics of the subcloud layer, except that outside the eyewall region we attempt to account, very crudely, for the crucial presence of downdrafts by reducing the entropy tendency there by a factor β.

The frontogenetical properties of (16) can be seen by differentiating it in R and making use of (13):

$$\frac{\partial V^2}{\partial \tau} = \frac{1}{2}R\frac{\partial}{\partial R}\left\{\frac{\beta}{\gamma}\left[V^3 - \frac{C_k}{C_D}V(\chi_s^* - \chi)\right]\right\}. \tag{17}$$

Ignoring variations in β/γ for the moment, (17) becomes

$$\frac{\partial V^2}{\partial \tau} = \frac{1}{2}\frac{\beta}{\gamma}R\left\{\left[3V^2 - \frac{C_k}{C_D}(\chi_s^* - \chi)\right]\frac{\partial V}{\partial R} - \frac{C_k}{C_D}V\frac{\partial}{\partial R}(\chi_s^* - \chi)\right\}. \tag{18}$$

The last term on the right-hand side of (18) usually damps the velocity, since $\chi_s^* - \chi$ generally increases with radius. This turns out to be always true at the radius of maximum wind. The first term on the right-hand side of (18) acts to propagate the V distribution across R surfaces at a phase speed given locally by

$$c = -\frac{1}{4}\frac{\beta}{\gamma}R\left[3V - \frac{1}{V}\frac{C_k}{C_D}(\chi_s^* - \chi)\right]. \tag{19}$$

Now, according to (19), the local phase speed in R space decreases with increasing V, so that *inside* the radius of maximum winds the gradient of V with respect to R will increase. By (15), the vorticity will eventually become infinite. Thus the eyewall flow is frontogenetic.

It is also apparent from (18), however, that the amplitude of V decreases in time. (At the potential radius of maximum winds, $\partial V/\partial R = 0$ and the remaining term turns out to be negative there.) How can the flow speed actually increase? Here we must emphasize the critical role of radial variations of β/γ. [Remember that β crudely represents the effects of subsaturation outside the eyewall. In point of fact, a major contributor to the subcloud-layer entropy balance outside the eyewall are the turbulent fluxes of entropy at the top of the subcloud layer (Rotunno and Emanuel 1987). These decrease the entropy tendency, and so $\beta < 1$ outside the eyewall.] Allowing for these, (17) becomes

$$\frac{\partial V^2}{\partial \tau} = \frac{1}{2}\frac{\beta}{\gamma}R\left[3V^2 - \frac{C_k}{C_D}(\chi_s^* - \chi)\right]\frac{\partial V}{\partial R} + \frac{1}{2}R\left[V^3 - \frac{C_k}{C_D}V(\chi_s^* - \chi)\right]\frac{\partial}{\partial R}\left(\frac{\beta}{\gamma}\right) - \frac{1}{2}R\frac{\beta}{\gamma}\frac{C_k}{C_D}V\frac{\partial}{\partial R}(\chi_s^* - \chi). \quad (20)$$

It follows from (20) that *the amplification of the wind speed in a hurricane depends on the existence of a negative gradient of β/γ at the radius of maximum winds,* since the first term on the right-hand side of (20) vanishes there and the last term is negative. In the model of Emanuel (1995a), γ is fixed and β always does decrease across the radius of maximum winds, principally because of convective downdrafts outside that radius. In a real hurricane, γ should increase across the radius of maximum winds since the depth of a rotationally constrained turbulent boundary layer is inversely proportional to the inertial stability, which is large inside the radius of maximum winds and small outside of it. This variation of γ also contributes, by (20), to amplification of the storm.

If we ignore the last term in (20), it is also clear that the maximum wind speed in the eyewall will be given by

$$V_m^2 = \frac{C_k}{C_D}(\chi_s^* - \chi)\big|_m, \quad (21)$$

which is identical to (8) [except that (8) is in dimensional form]. Not surprisingly, the dynamics give the same answer as that obtained from consideration of the energetics.

We have seen that the eyewall dynamics are frontogenetic and that they imply maximum wind speeds that are in good agreement with those produced in numerical simulations (Fig. 4). But the simple model here does not encompass the special dynamics of the hurricane eye, where subsidence produces temperatures well in excess of those produced by lifting boundary layer air. The lack of eye dynamics can be seen by referring back to (16) and noticing that the two terms on the right-hand side of (16) are proportional to $\partial\chi/\partial R$ and $\sqrt{\partial x/\partial R}$ respectively, by (13). *Thus (16) allows no amplification of the χ field,* even though the swirling velocity may amplify. Since V^2 is always positive and, by (13), proportional to $-\partial\chi/\partial R$, χ must reach its maximum value at $R = 0$, but there is no mechanism for χ to change at $R = 0$.

Part of the problem may result from neglecting $1/r_t^2$ in (9), which is tantamount to assuming zero absolute vorticity at the tropopause. Inside the R surface along which the vertical velocity is a maximum, mass continuity implies radially inward motion at high levels, leading to a decrease in r_t. If the cyclonic vorticity at the tropopause attains a value *much* greater than the Coriolis parameter, then (16) may be approximated by

$$V^2 \simeq V_t^2 - \frac{1}{2}R\frac{\partial \chi}{\partial R}, \quad (22)$$

where V_t is the azimuthal velocity at the tropopause. Using (22) for V in (16) shows that amplification of the χ field is now possible through the surface fluxes. This demonstrates that the upper boundary condition can play an important role in the hurricane dynamics and, in particular, that external influences that increase the cyclonic flow at the tropopause near the core (such as interaction with cyclonic potential vorticity anomalies, as suggested by Molinari et al. 1995) can intensify the system.

Yet axisymmetric numerical models with no external influences have no trouble producing an amplification of both the χ and V fields. It is well known that eye subsidence is effective in increasing the temperature there; this is essential for allowing the temperature field to amplify in concert with V. The subsidence acts to decouple the free atmosphere temperature field from the boundary layer entropy, χ. There are two mechanisms for warming the eye: convectively induced subsidence owing to convective heating in the eyewall (Shapiro and Willoughby 1982) and mechanically forced subsidence owing to the spinup of the eye by radial stress from the eyewall (Smith 1980). Here is a brief review of these mechanisms.

The convectively induced warming may be considered in relation to the fact that, even in a hurricane, convective updrafts cover a small fractional area. The dynamics of rotating stratified fluids dictates that temperature perturbations be spread over a horizontal scale proportional to the local deformation radius. As shown by Shapiro and Willoughby (1982), this implies (through a Sawyer–Eliassen-type equation in circular coordinates) a rather strong secondary circulation outside the eyewall with a weaker circulation in the eye. This circulation is, in most models, thermally direct for at least a short time during the initial spinup. For the present purposes, it is important to note that *these convectively induced secondary circulations cannot by themselves raise the vertically averaged temperature to a value greater than that inside convective clouds.* The proof of this is contained in the appendix. Thus the convectively driven secondary circulation can, at most, cause the average saturation entropy χ^* in the eye to equal its value in the eyewall. This component of the secondary circulation cannot, therefore, solve the problem of lack of amplification of the χ field. From (13), it is evident that when χ^* is uniform in the eye, V is zero there.

Note also that subsidence in the eye must be associated with divergence near the base of the eye. Thus the convective circulations alone cannot directly spin up the eye circulation. The only process that can do this is turbulent fluxes of momentum from the eyewall (Malkus 1958; Kuo 1958). Three-dimensional turbulence has the effect of driving the eye circulation toward

a state of solid-body rotation; turbulence of this kind is represented parametrically in virtually all extant numerical simulations. In the steady state, the inward flux of angular momentum by turbulence in the eye must balance the downward turbulent flux of angular momentum into the sea surface; thus a concave velocity profile (outward-increasing angular velocity) is required, though the concavity may be slight.

As pointed out by Smith (1980), the outward slope of the eyewall together with near solid-body rotation in the eye implies that the eye circulation decreases with altitude; this in turn implies, through the thermal wind relation, that the temperature must increase radially inward along pressure surfaces. The radial temperature gradient inside the eye is a by-product of the mechanical spin up of the eye by the eyewall.

Unlike convectively induced subsidence, the subsidence forced by the mechanical spinup of the eye can actually amplify the χ^* field beyond the value of χ in the eyewall. This is because, through the thermal wind relation (13), mechanical spinup of the eye must necessarily lead to an inward increase in χ^* to maintain thermal wind balance. It does so through subsidence forced by the eddy momentum fluxes. We conclude that *the mechanical spinup of the eye by radial stress with the eyewall is crucial for amplification of the entropy distribution in hurricanes,* even though it is *not* necessary for amplification of the wind field.

We attempt to illustrate these deductions about the dynamics of the hurricane core through the use of three very simple models. All three models use (16) for calculating the boundary layer entropy distribution. As we have seen, a negative gradient of β/γ across the radius of maximum winds is necessary for amplification of the wind field, though the maximum wind speed is independent of β/γ. For simplicity, we take β/γ to be unity inside the radius of maximum winds and zero outside of it. (The choice of unity is arbitrary; any other value can be absorbed into the scaling of time. Taking β to be nonzero outside the eyewall results in a weak tendency of χ there, even after maximum intensity is reached, but does not affect the qualitative conclusions that follow. Also, for reasons of numerical stability, we actually allow β/γ to decrease smoothly from unity to zero over a range of eight grid points straddling the radius of maximum winds. This specification of β/γ does no justice to the dynamics outside the eyewall, where the actual χ^* distribution is determined by the dynamically set distribution of subsidence and by boundary layer thermodynamics, including convective downdrafts. This simplification stems from the desire to focus on the eyewall dynamics and to allow for the possibility of strictly steady solutions, and does not affect the qualitative conclusions derived from these very simple models.) The thermal wind relation (13) is assumed to hold everywhere, though for generality we must replace the entropy χ by the saturation entropy χ^* to include cases where the air is conditionally stable (i.e., the eye, where $\chi^* > \chi$):

$$V^2 = -\frac{R}{2}\frac{\partial \chi^*}{\partial R}.^2 \tag{23}$$

In the first of the three models, which we call the ''zero diffusion'' model, we assume that there is no mechanical spinup of the eye, and that the convectively induced subsidence results in an eye temperature that is uniform on pressure surfaces and always equal to the value of χ (and thus χ^*) in the eyewall. Since χ^* is thus horizontally uniform in the eye, $V = 0$ there by virtue of (23). This is consistent with the assumed absence of viscous stresses in this model of the eye. For simplicity, we take the inner edge of the eyewall to be the radius at which the boundary layer value of χ is a maximum. Thus, in this very simple model,

$$\chi^* = \begin{cases} \chi & R \geq R_{\chi_{\max}}, \\ \chi_{\max} & R < R_{\chi_{\max}}, \end{cases} \tag{24}$$

where $\chi_{\max}$ is the maximum value of χ in the boundary layer and $R_{\chi max}$ is the potential radius at which this maximum occurs.

To close the model, the saturation entropy of the sea surface that appears in (16) must be specified. We linearize the dependence of the saturation entropy on pressure, giving

$$\chi_s^* \simeq 1 - AP \simeq 1 + A\left(\chi^* + \frac{1}{2}V^2\right), \tag{25}$$

following Emanuel (1995a), where the definition of the coefficient A may be found. (Its value is typically near 0.5.)

Thus the first of these highly simplified models consists of (16) and (23)–(25), with β/γ varying from unity inside the radius of maximum winds to zero outside of it. [We add a small amount of damping to (16) to control the numerical integration.] Nothing in this model prevents frontal collapse, as indicated by (15), and indeed a discontinuity forms in a small amount of time. For this reason, we display, in Fig. 6, the fields in potential radius (R) coordinates instead of physical space. It is clearly seen that the azimuthal velocity amplifies toward its maximum value, while the amplitude of the χ field changes little. (What change does occur is caused by some numerical noise.) Once again, this model produces just enough subsidence in the eye to keep its temperature equal to the eyewall temperature on each pressure surface, consistent with zero azimuthal velocity throughout the eye, since there is no mechanism to spin up the eye.

[2] In regions of subsidence, there is no reason for χ^* to be uniform along angular momentum surfaces. Assuming it to be so is analogous to assuming constant background stratification in the quasigeostrophic system.

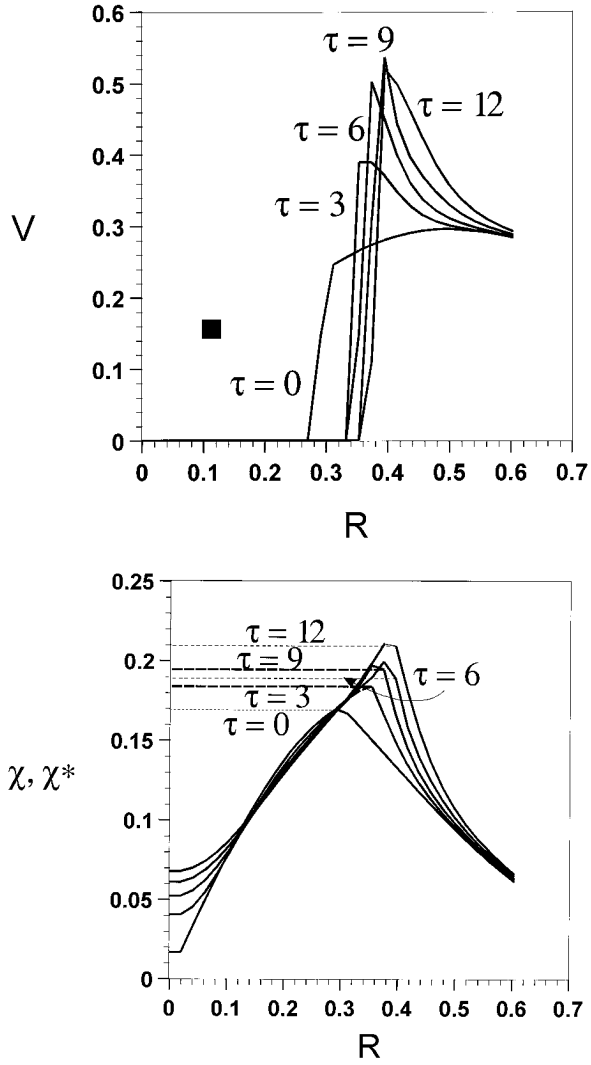

FIG. 6. (a) Dimensionless swirling velocity and (b) entropy as a function of potential radius, at 5 times, in the zero diffusion model. In (b), the dashed lines show the saturation entropy of the free atmosphere.

Were Fig. 6 drawn in physical coordinates, both fields would be folded starting shortly after the initial time.

The breakdown of this model at the time of formation of a discontinuity leads us to propose a second model, which will be referred to as the ''minimum diffusion'' model. It contains just enough diffusion to prevent the model fields from going beyond a pure discontinuity, as indicated by (15). From (15), we insist that

$$\frac{\partial V}{\partial R} \leq \frac{R}{r}.$$

Using (12) to eliminate r, this gives

$$\frac{\partial V}{\partial R} \leq \frac{2V}{R}. \tag{26}$$

We apply (26) by insisting that inside the outermost radius at which (26) is violated,

$$V = V_{crit}\left(\frac{R}{R_{crit}}\right)^2, \tag{27}$$

where V_{crit} is the wind speed at R_{crit}, which is the maximum potential radius at which (26) is violated. This has the effect of adjusting the gradient of V back to its critical value given by (26). Integrating (23) inward from R_{Vm} using (27) gives

$$\chi^* = \begin{cases} \chi & R \geq R_{crit}, \\ \chi_{crit} + \dfrac{1}{2}V_{crit}^2\left[1 - \left(\dfrac{R}{R_{crit}}\right)^4\right] & R < R_{crit}. \end{cases} \tag{28}$$

The saturation entropy at the storm center is amplified over the eyewall entropy by a factor of $1/2V_{crit}^2$.

The second model, then, consists of (16), (23), (25), and (28) with β/γ varying as before. The results of integrating this model are shown in Fig. 7, and this time the fields are displayed in physical space. As dictated by the design of the experiment, the vorticity is infinite in the eyewall. [The velocity would be exactly zero in the eye, but to transform to physical space we have used the full back-transform from (10), whereas (15) is based on the approximation that the vorticity is much larger than the Coriolis parameter.]

In this second experiment, the V, χ, and χ^* fields all amplify, and the V field amplifies substantially faster and to a greater amplitude than in the first experiment. One reason for this is that the radial diffusion increases the swirling velocity inside the critical radius (in R space) and thus increases the surface entropy flux there. This in turn increases the entropy inside the radius of maximum winds and thus helps increase the negative gradient of χ^*, which is proportional to V^2, at the radius of maximum winds. The momentum diffusion thus has a positive feedback on the velocities through its effect on the surface heat fluxes. The rate of development in this simple model is probably overestimated owing to the neglect of radial diffusion of heat.

We emphasize that the first model becomes ill posed at the time of formation of an actual discontinuity, so that this second model represents the minimum diffusion that leads to physically possible solutions after formation of the discontinuity. In effect, frontal formation creates a circumstance in which mechanical diffusion *must* occur and *must* lead to a jump in χ^* across the radius of maximum winds. This suggests a critical role of eyewall frontogenesis in allowing for amplification of the entropy field in hurricanes, at least once the upper anticyclone is fully developed ($r_t \to \infty$).

In the third model, called the ''maximum diffusion'' model, we assume that three-dimensional turbulence is perfectly efficient in establishing uniform angular velocity (solid-body rotation) inside the radius of maxi-

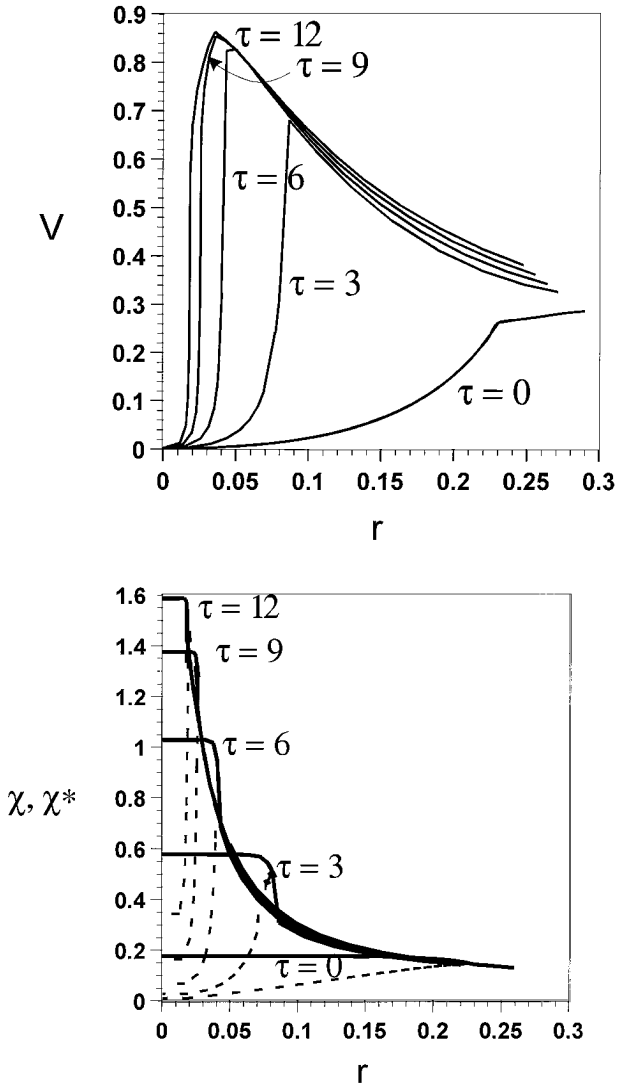

FIG. 7. As in Fig. 6 but for the minimum diffusion model shown as a function of physical radius. In this case, the dashed lines show the boundary layer entropy, while the full lines show the saturation entropy of the free atmosphere.

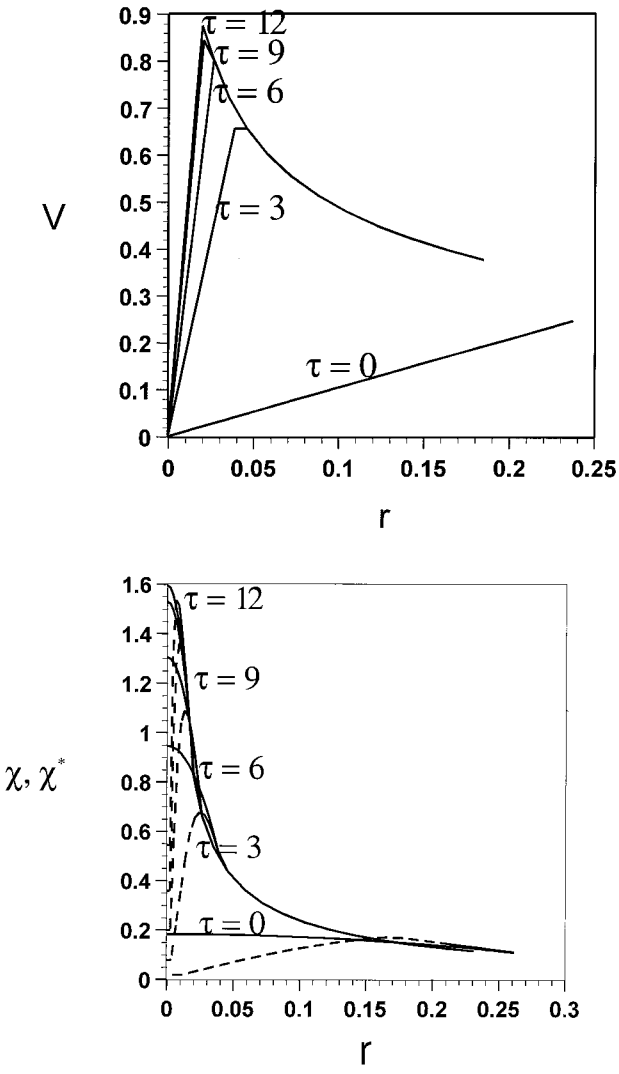

FIG. 8. As in Fig. 7 but for the maximum diffusion model.

mum winds. (But, again, we neglect diffusion of heat.) Thus we assume that inside the radius of maximum winds,

$$V = V_m\left(\frac{r}{r_{v_m}}\right) = V_m\left(\frac{R}{R_{V_m}}\right), \tag{29}$$

where r_{Vm} is the physical radius of maximum winds, and the second equality results from the first in combination with (10). In adjusting the momentum field, we insist upon global conservation of angular momentum, so that the quantity

$$\int_0^{r_m} Vr^2\, dr$$

is conserved during the adjustment. Integrating (23) gives

$$\chi^* = \begin{cases} \chi, & R \geq R_{V_m}, \\ \chi_m + V_m^2\left[1 - \left(\dfrac{R}{R_{V_m}}\right)^2\right], & R < R_{V_m}. \end{cases} \tag{30}$$

The saturation entropy at the storm center is amplified over the eyewall entropy by a factor of V_m^2, twice the value of the minimum diffusion model. The third model, then, consists of (16), (23), (25), and (30), with β/γ varying as before. The results of integrating this model are displayed in Fig. 8. The swirling velocity amplifies at about the same rate as in the minimum diffusion model, but the eye temperature (proportional to χ^*) is somewhat higher. This corresponds to lower central pressure, reflecting the additional swirling velocity in

the eye. Once again, momentum diffusion has the positive feedback effect of increasing the surface entropy fluxes inside the radius of maximum winds, but the additional surface dissipation in the eye leads to a slightly smaller maximum wind speed than in the second model.

These three models, taken together with previous research results, suggest that the intensification of tropical cyclones may be usefully divided into two stages. The first stage is defined to encompass the evolution of the system before eyewall frontal collapse has occurred. We hypothesize that two critical circumstances must occur during the first stage: a mesoscale column or ring of nearly saturated air must be established, and a positive anomaly of entropy (θ_e) must develop in the subcloud layer. The three models described in this section presuppose that these events have taken place. As shown previously (Rotunno and Emanuel 1987; Emanuel 1989), the near-saturation condition is critical; otherwise, ascent leads to convective downdrafts that decrease the subcloud-layer entropy and quench the development. (This effect is not included in the simple models presented in this section, except implicitly in the specification of β.) Here it has been shown that *the WISHE mechanism cannot by itself amplify the subcloud-layer entropy distribution once the upper anticyclone is fully developed* ($r_t \to \infty$) *and before frontal collapse occurs.* This suggests an important role for interaction with external systems in the upper troposphere, insofar as they diminish anticyclonic vorticity near the tropopause, as has been shown observationally by Molinari et al. (1995). The downward projection of the cyclonic vorticity along angular momentum surfaces, which act as characteristic surfaces in moist potential vorticity inversion, yields a component of surface wind that may be in phase with the subcloud-layer entropy distribution, allowing the latter to amplify through surface entropy fluxes.

The system dynamics undergo a strong transition when frontal collapse occurs at the eyewall. Even in the inviscid limit, radial diffusion becomes important and leads to strong subsidence in the eye, enough to increase the saturation entropy of the eye over that of the eyewall by a factor of $1/2V_m^2$ (in nondimensional terms). Before radial diffusion of momentum becomes important, the vertically averaged saturation entropy of the central region is limited to a value no larger than that of the entropy of the eyewall. We emphasize that convection alone cannot cause the temperature to exceed the vertically averaged temperature inside the convective clouds, except transiently in association with gravity waves.

Although the wind field can amplify in the absence of the frontal dynamics, the entropy distribution apparently cannot amplify in the absence of both frontal dynamics and upper tropospheric influences. Frontal formation allows both fields to amplify in concert, and the wind field amplifies somewhat more rapidly than in the case in which the frontal dynamics are ignored.

After frontal collapse has taken place, radial momentum diffusion may be expected to slowly establish a swirling velocity profile that is near solid body rotation, but at least slightly concave to allow an inward turbulent flux of angular momentum to compensate frictional loss at the sea surface. By thermal wind balance, this leads to an additional increase of saturation entropy of $1/2V_m^2$ at the storm center; to accomplish this, there must be additional subsidence. This additional subsidence is mechanically forced by the spinup of the eye by the eyewall. When a quasi-steady state is reached, there will be some continual subsidence owing to radiative cooling and, secondarily, by some outward turbulent diffusion of heat that may occur as a by-product of the inward turbulent diffusion of angular momentum. This basic balance of the mature eye, with inward turbulent diffusion of angular momentum balancing loss to the surface and outward turbulent diffusion of heat and radiative cooling balancing subsidence warming, was found in numerical simulations by Kurihara and Bender (1982).

The pivotal role of radial turbulent momentum diffusion in the intensification of hurricanes is also suggested in numerical simulations using potential radius as the radial coordinate. The author (Emanuel 1989) used such a model to perform an experiment in which the explicit radial diffusion of angular velocity was turned off but radial heat diffusion was retained. In contrast to a control experiment with equal coefficients of angular velocity and heat diffusion, the wind field in this experiment experienced only very slow intensification after frontal collapse (see Fig. 5 of that paper). Given equal coefficients of angular velocity and heat diffusion, the same model's behavior is quite insensitive to the magnitude of the coefficients.

4. Summary

The analysis undertaken here suggests an answer to Willoughby's question, quoted in the introduction. Given an initial positive entropy anomaly in the subcloud layer, and a mesoscale column or ring of nearly saturated air collocated with it, the wind field can apparently amplify in the absence of the special dynamics associated with the eye. By ''special dynamics'' we mean, specifically, the strong, radial turbulent diffusion of momentum that is responsible for the spinup of the eye. But without such diffusion, the WISHE mechanism is incapable of amplifying the entropy distribution of the storm, unless interaction with external dynamical systems results in an increase of vorticity near the tropopause. The *radial gradient* of the entropy does amplify in concert with the swirling velocity. Convectively forced subsidence in the eye can do no more than keep the vertically averaged eye temperature equilibrated to that of the eyewall.

But we have shown here that the amplification of the swirling flow is strongly frontogenetic and results, in a

comparatively short time, in frontal collapse at the inner edge of the eyewall. This frontal collapse leads to a dramatic transition in the storm dynamics. Once it has occurred, radial turbulent diffusion of momentum *must* become important, even in the inviscid limit, and it necessarily results in a mechanically induced, thermally indirect component of the secondary circulation in the eye and eyewall. Such a circulation raises the vertically averaged temperature of the eye beyond its value in the eyewall and allows for an amplification of the entropy distribution. Feedbacks with the surface fluxes then allow the boundary layer entropy to increase and also result in a more rapid intensification of the swirling wind.

Thus, we argue that frontal collapse of the eyewall is a key process in the evolution of tropical cyclones. Without it, amplification of the temperature distribution relies on external influences and intensification of the wind field is slow. Once it has taken place, the mechanical spinup of the eye allows the temperature distribution to amplify without external influences and, through positive feedback with surface fluxes, allows the entropy field to amplify and the swirling velocity to increase somewhat more rapidly. With or without frontogenesis, the maximum wind speed is set by the energy available from the Carnot cycle.

Acknowledgments. The author thanks Drs. Hough Willoughby, Greg Holland, and Roger Smith for the insightful comments that led to many improvements in this work, which was supported by the National Science Foundation under Grant 9320445-ATM.

APPENDIX

Proof That Convection Cannot Cause the Vertically Averaged Temperature to Exceed That in Convective Clouds in a Balanced Model

The proof stems from an elliptic equation for the pressure tendency in cylindrical coordinates for flow in hydrostatic and gradient balance. All the equations here involve dimensionless variables, phrased in potential radius coordinates. The potential radius R is given by

$$R^2 = 2rV + r^2. \tag{A1}$$

The independent variables in this system are R, pressure (P), and time (τ); partial derivatives with respect to one of these assume that the other two are held fixed.

In these coordinates, the gradient wind and hydrostatic equations may be written as (see footnote 2 of Schubert and Hack 1983)

$$\frac{1}{r^2} = \frac{1}{R^2} + \frac{2}{R^3}\frac{\partial \Phi}{\partial R} \tag{A2}$$

and

$$\theta = -\frac{\partial \Phi}{\partial P}\frac{\partial P}{\partial \pi}, \tag{A3}$$

where θ is the potential temperature, π is the Exner function [$= c_p(P/P_0)^{R_d c_p}$, where c_p is the heat capacity at constant pressure, R_d is the gas constant, and P_0 is a reference pressure], and Φ is the modified geopotential

$$\Phi = \varphi + \frac{1}{2}V^2,$$

where φ is the actual geopotential.

The thermodynamic equation (see also Schubert and Hack 1983; Emanuel 1989) is

$$\frac{\partial \theta}{\partial \tau} = Q - \frac{1}{2\sigma R}\frac{\partial \psi}{\partial R}, \tag{A4}$$

where Q is a dimensionless heating rate, ψ is the mass streamfunction, and σ is the inverse potential vorticity. Finally, the mass continuity equation may be written as (Emanuel 1989)

$$\frac{\partial r^2}{\partial \tau} = \frac{\partial \psi}{\partial P}. \tag{A5}$$

An elliptic equation relating the local time tendency of the modified geopotential Φ to the heating Q can be derived as follows. First, differentiate (A2) in time and then use (A5) to eliminate $\partial r^2/\partial \tau$. The result is

$$\frac{\partial \psi}{\partial P} = -\frac{2r^4}{R^3}\frac{\partial}{\partial R}\frac{\partial \Phi}{\partial \tau}. \tag{A6}$$

Next, multiply (A4) through by σ and substitute (A3) for θ:

$$\frac{1}{2R}\frac{\partial \psi}{\partial R} = \sigma Q + \sigma\frac{dP}{d\pi}\frac{\partial}{\partial P}\frac{\partial \Phi}{\partial \tau}. \tag{A7}$$

Finally, eliminate ψ between (A6) and (A7), giving

$$\frac{1}{R}\frac{\partial}{\partial R}\left(\frac{r^4}{R^3}\frac{\partial}{\partial R}\frac{\partial \Phi}{\partial \tau}\right) + \frac{\partial}{\partial P}\left(\sigma\frac{dP}{d\pi}\frac{\partial}{\partial P}\frac{\partial \Phi}{\partial \tau}\right) = -\frac{\partial}{\partial P}(\sigma Q). \tag{A8}$$

It can be easily demonstrated, using (A8), that the geopotential tendency has no extremum in any place where $Q = 0$, other than perhaps at a boundary.[3] First, expand the derivations on the left-hand side of (A8) in any place where $Q = 0$:

$$\frac{1}{R}\frac{\partial}{\partial R}\left(\frac{r^4}{R^3}\right)\frac{\partial}{\partial R}\frac{\partial \Phi}{\partial \tau} + \frac{\partial}{\partial P}\left(\sigma\frac{dP}{d\pi}\right)\frac{\partial}{\partial P}\frac{\partial \Phi}{\partial \tau} + \frac{r^4}{R^4}\frac{\partial^2}{\partial R^2}\frac{\partial \Phi}{\partial \tau} + \sigma\frac{dP}{d\pi}\frac{\partial^2}{\partial P^2}\frac{\partial \Phi}{\partial \tau} = 0. \tag{A9}$$

For there to be an extremum of $\partial\Phi/\partial\tau$ away from boundaries, three conditions must be satisfied:

[3] If the boundary can be represented by image heat sources that are not themselves at the boundary, then (A8) implies that no extremum of geopotential tendency can occur in any place where $Q = 0$.

$$\frac{\partial}{\partial R}\frac{\partial \Phi}{\partial \tau} = 0,$$

$$\frac{\partial}{\partial P}\frac{\partial \Phi}{\partial T} = 0, \qquad \left(\frac{\partial^2}{\partial R^2}\frac{\partial \Phi}{\partial \tau}\right)\left(\frac{\partial^2}{\partial P^2}\frac{\partial \Phi}{\partial \tau}\right) > 0. \quad \text{(A10)}$$

The last condition ensures that the curvatures of the distribution of $\partial\Phi/\partial\tau$ in both directions have the same sign. Examination of (A9) shows that, provided σ is everywhere positive, the conditions (A10) cannot all be satisfied. Thus, $\partial\Phi/\partial\tau$ cannot have an extremum where $Q = 0$ other than at a boundary that is not representable by image heat sources.

Now consider a localized heat source and integrate (A3), starting a sufficient distance from the source that there can be considered to be no geopotential tendency there. The result is

$$\Phi = \int_{\infty}^{P} \frac{d\pi}{dP}\theta \, dp = \int_{\infty}^{P} RT \, d \, \ln P, \quad \text{(A11)}$$

where we have used the definition of the Exner function π. Differentiating in time gives

$$\frac{\partial \Phi}{\partial \tau} = \int_{\infty}^{P} R\frac{\partial T}{\partial \tau} \, d \, \ln P. \quad \text{(A12)}$$

Suppose we take the limit of integration (P) in (A12) to be just above where a single point source of heat is located [where $\partial/\partial P(\sigma Q)$ is a maximum]. It follows from the aforementioned results that *the extreme value of the integral in (A12) will be found along that R surface that intersects the heat source.*

Here it is important to recognize that, in the atmosphere, the heat source is not specified; it is internal. Whatever else may be said about convection, it will not proceed if the virtual temperature of a parcel lifted adiabatically from the subcloud layer is less than that of its immediate environment. We have established that the tendency of temperature averaged vertically along angular momentum surfaces is always maximized at the angular momentum surface(s) containing the heat source(s). As soon as the (virtual) temperature increases to that of an adiabatically lifted parcel, the convection will cease. It follows that *convection cannot, by itself, raise the temperature averaged vertically along angular momentum surfaces to a value higher than that of an adiabatically lifted parcel, given a balanced flow with nonnegative potential vorticity.*

This statement should not be taken to preclude the ability of convection to further increase temperature *where it is already higher than that of convective clouds.* If some other process (e.g., angular momentum diffusion) creates an eye that is warmer than the air inside convective clouds, the circulation induced by the clouds can make it warmer still. Even in this case, though, the *rate* of warming caused directly by the clouds will be largest next to the convective clouds, so eventually the eyewall temperature would overtake the eye temperature were it not for the action of other processes.

REFERENCES

Eliassen, A., 1959: On the formation of fronts in the atmosphere. *The Atmosphere and Sea in Motion,* B. Bolin, Ed., Oxford University Press, 227–287.

Emanuel, K. A., 1986: An air–sea interaction theory for tropical cyclones. Part I: Steady-state maintenance. *J. Atmos. Sci.,* **43,** 585–604.

——, 1988: The maximum intensity of hurricanes. *J. Atmos. Sci.,* **45,** 1143–1155.

——, 1989: The finite-amplitude nature of tropical cyclogenesis. *J. Atmos. Sci.,* **46,** 3431–3456.

——, 1995a: The behavior of a simple hurricane model using a convective scheme based on subcloud-layer entropy equilibrium. *J. Atmos. Sci.,* **52,** 3960–3968.

——, 1995b: Sensitivity of tropical cyclones to surface exchange coefficients and a revised steady-state model incorporating eye dynamics. *J. Atmos. Sci.,* **52,** 3969–3976.

Hawkins, H. F., and S. M. Imbembo, 1976: The structure of a small, intense hurricane—Inez, 1966. *Mon. Wea. Rev.,* **104,** 418–442.

Hoskins, B. J., and F. P. Bretherton, 1972: Atmospheric frontogenesis models: Mathematical formulation and solution. *J. Atmos. Sci.,* **29,** 11–37.

Kleinschmidt, E., 1951: Grundlagen einer Theorie der Tropischen Zyklonen. *Arch. Meteorol. Geophys. Bioklimatol.,* **A4,** 53–72.

Kuo, H.-L., 1958: Dynamics of convective vortices and eye formation. *The Atmosphere and Sea in Motion,* B. Bolin, Ed., Rockefeller Institute Press, 413–424.

Kurihara, Y., and M. Bender, 1982: Structure and analysis of the eye of a numerically simulated tropical cyclone. *J. Meteor. Soc. Japan,* **60,** 381–395.

Malkus, J. S., 1958: On the structure of the mature hurricane eye. *J. Meteor.,* **15,** 337–349.

Miller, B. I., 1958: On the maximum intensity of hurricanes. *J. Meteor.,* **15,** 184–195.

Molinari, J., S. Skubis, and D. Vollaro, 1995: External influences on hurricane intensity. Part III: Potential vorticity structure. *J. Atmos. Sci.,* **52,** 3593–3606.

Ooyama, K., 1969: Numerical simulation of the life-cycle of tropical cyclones. *J. Atmos. Sci.,* **26,** 3–40.

Palmén, E., and C. W. Newton, 1969: *Atmospheric Circulation Systems.* Academic Press, 603 pp.

Riehl, H., 1950: A model for hurricane formation. *J. Appl. Phys.,* **21,** 917–925.

——, 1954: *Tropical Meteorology.* McGraw-Hill, 392 pp.

Rosenthal, S. L., 1971: The response of a tropical cyclone model to variations in boundary layer parameters, initial conditions, lateral boundary conditions, and domain size. *Mon. Wea. Rev.,* **99,** 767–777.

Rotunno, R., and K. A. Emanuel, 1987: An air–sea interaction theory for tropical cyclones. Part II: Evolutionary study using a nonhydrostatic axisymmetric numerical model. *J. Atmos. Sci.,* **44,** 542–561.

Schubert, W. H., and J. J. Hack, 1983: Transformed Eliassen balanced vortex model. *J. Atmos. Sci.,* **40,** 1571–1583.

Shapiro, L. J., and H. E. Willoughby, 1982: The response of balanced hurricanes to local sources of heat and momentum. *J. Atmos. Sci.,* **39,** 378–394.

Smith, R. K., 1980: Tropical cyclone eye dynamics. *J. Atmos. Sci.,* **37,** 1227–1232.

Willoughby, H. E., 1995: Eye thermodynamics. Preprints, *21st Conf. on Hurricanes and Tropical Meteorology,* Miami, FL, Amer. Meteor. Soc., 357–358.